
Proceedings Paper:

Maddi, C, Aswin, JR, Adarsh, KV et al. (2 more authors) (2019) Spectroscopic and Structural Properties of Yb3+-Doped and Undoped 2D-Mos2 Thin Films for Optoelectronic and Photonic Device Applications. In: 2019 Conference on Lasers and Electro-Optics Europe and European Quantum Electronics Conference, CLEO/Europe-EQEC 2019. CLEO/Europe-EQEC 2019, 23-27 Jun 2019, Munich, Germany. IEEE . ISBN 9781728104690

https://doi.org/10.1109/CLEOE-EQEC.2019.8872550

Supporting information

Structural, Spectroscopic, and Excitonic Dynamic Characterisation in atomically thin Yb^{3+} -doped MoS_2, fabricated by femtosecond pulsed laser deposition

Chiranjeevi Maddi[1], J R Aswin[2], Andrew J Scott [1], Zabeada Aslam[1], Elizabeth A Willneff [3], K. V Adarsh [2], Animesh Jha[1*]

[1]School of Chemical and Process Engineering, Faculty of Engineering, University of Leeds, Leeds LS2 9JT, UK

[2]Department of Physics, Indian Institute for Science Education and Research (IISER), IISER Bhopal, India

[3]School of Design, Faculty of Arts, Humanities and Cultures, University of Leeds, Leeds LS2 9JT UK

Corresponding Authors[*+]

[*]Email: a.jha@leeds.ac.uk

[+]Email: kv.adarsh@gmail.com

Raman Spectroscopy:

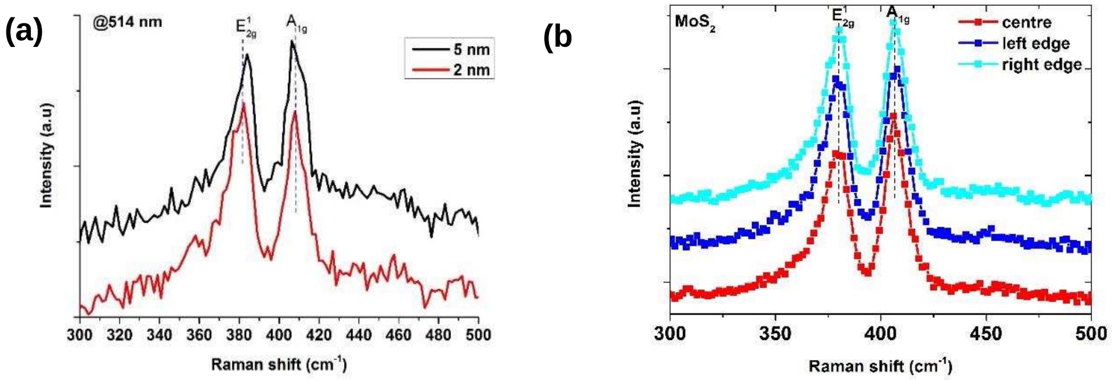

Figure S1: Raman spectra of MoS_2 at excitation wavelength 514 nm: (a) thickness dependent, (b) uniform film thickness measurements.

X-Ray Photoelectron Spectroscopy (XPS):

(a)

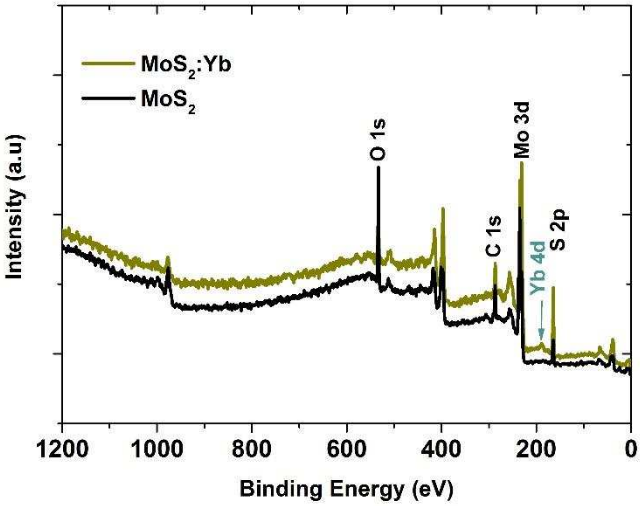

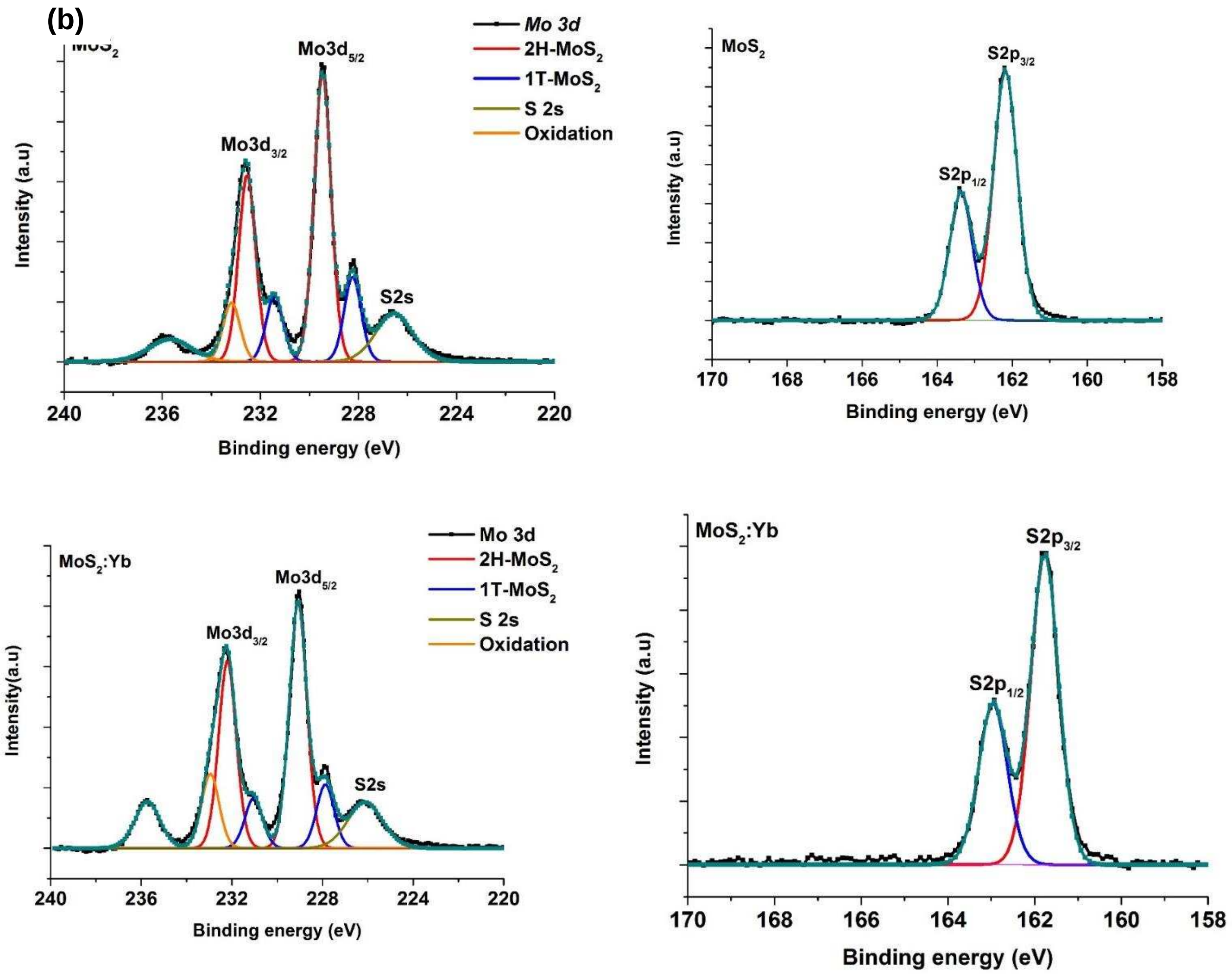

Figure S2: XPS of MoS$_2$: (a) General scan spectra of undoped and Yb^{3+} doped MoS$_2$, (b) Comparison of Molybdenum (Mo) and Sulfer (S) core level XPS data for undoped and Yb^{3+}-ion doped MoS$_2$ films.

The chemical composition and doping were estimated by using X-ray photoelectron spectroscopy (XPS). Figure S2 a-e shows the survey scan, Mo 3d, S2s and S2p regions of the undoped and Yb doped MoS$_2$ samples. Figure S2 (a) shows the comparison of the general scan spectra of MoS$_2$ and doped MoS$_2$. Figure S2 (b) shows the comparison of XPS Mo3d core level spectra of MoS$_2$ and Yb-doped MoS$_2$. It is observed that the core level spectra of Mo and S in the MoS$_2$:Yb sample present a uniform shift towards the lower binding energies by ~0.3-0.4 eV with respect to the peak position of 2H-$MoS_2$of undoped MoS_2. Such a shift in binding energy indicates the change in the chemical microenvironment of doped samples, the Fermi level shift is a clear indication of doping of Yb into Mo lattice. The Mo 3d spectra consist of peaks at around 229.47 eV and 232.54 eV corresponding to $Mo^{4+}3d_{5/2}$ and $Mo^{4+}3d_{3/2}$ spin orbital doublet associated with 2H-MoS_2 phase, respectively. Figure S2b shows the deconvolution of Mo3d spectra of undoped MoS_2 film. The deconvoluted Mo3d spectra of undoped MoS_2 reveal additional peaks which are located at 228.23 eV and 231.44 eV ascribed to 1T-MoS_2 phase, and peaks at 233.18 eV and 235.80 eV associated with the oxidation state. Similarly, the deconvoluted S2p spectra consist of peaks at around 162.19 eV and 163.38 eV corresponding to S $2p_{3/2}$ and S $2p_{1/2}$ in undoped MoS_2 film showed in Figure S2 c. Figure S2 d and Figure S2 e show the deconvolution of Mo3d and S 2p of Yb doped MoS_2 films. These films show four distinct features; peaks at 229.05 eV and 232.20 eV corresponding to $Mo^{4+}3d_{5/2}$ and $Mo^{4+}3d_{3/2}$ components of 2H-MoS_2, peaks at 227.88 eV and 231.03 eV ascribed to 1T-MoS_2, and peaks at 232.94 eV and 235.67 eV associated with the oxidation states. The deconvoluted S 2p valence spectra (Figure S2 e) of doped MoS_2 consist of doublet peaks at around 161.76 eV and 162.94 eV corresponding to S $2p_{3/2}$and S $2p_{1/2}$, respectively. When the films were compared with respect to other, the peaks shifted to lower binding energies in Yb doped MoS2 than in doped MoS2. The shift may be attributed to the switch from n-type to p-type conductivity with Yb doping. In order to confirm the type of doping, we need further characterizations of the films. [1-3].

Table S1: Comparison of Mo and S core level binding energy values of undoped and Yb^{3+} doped MoS2 films.

	2H-MoS$_2$ BE, eV	1T-MoS$_2$ BE, eV	1T –MoS$_2$ BE, eV	S2s BE, eV	S2p3/2 BE, eV	S2p1/2 BE, eV
MoS2	**Mo3d5/2: 229.47** **Mo3d3/2: 232.54**	**Mo3d5/2: 228.23** **Mo3d3/2: 231.44**	**Mo3d5/2: 233.18** **Mo3d3/2: 235.80**	**226.55**	**162.19**	**163.38**
MoS2:Yb	**Mo3d5/2: 229.05** **Mo3d3/2: 232.20**	**Mo3d5/2: 227.88** **Mo3d3/2: 231.03**	**Mo3d5/2: 232.94** **Mo3d3/2: 235.67**	**226.13**	**161.76**	**162.94**

Table S2: A comparison of the calculated lattice parameters and relative energies of the 2H and 1T allotropes of MoS$_2$.

MoS$_2$ (bulk)	Space group Crystal system	a (Å)	c (Å)	Mo-S (Å)	ΔE (kJ/ mol.fu) (kJ/mol.atom)
2H	P6$_3$/mmc Hexagonal	3.1587 (+0.1%)	12.0872 (-1.4%)	2.401	0 0
1T	P-3m Trigonal	3.1957 (+0.2%)	5.6432 (-5.1%)	2.418	+76.1 +25.4

Band structure calculation (Hybrid functional):

The electronic structure of molybdenum disulfide (MoS$_2$) was analysed through the first principles calculations using density functional theory (DFT) using CASTEP code. DFT is known to significantly underestimate the bandgap in materials; therefore we have used a recent computationally intensive hybrid functional (HSE06) code, which is able to predict the bandgap accurately. Bulk MoS$_2$ was geometry optimised (dispersion corrected TS-PBE functional) giving a=3.159 A°(~0.1%) and c=12.071 A° (~1.8%). A monolayer of MoS$_2$ was modelled using a supercell with an interplanar (vacuum) distance of 15 A° to avoid interactions between adjacent sheets. DFT calculations accurately predict the expected increase in the bandgap from bulk MoS$_2$ (1.26 eV indirect) to monolayer MoS$_2$ (~2.27 eV direct). Indirect bandgap of monolayer

MoS_2 lies between point Γ to Γ-K in first Brillouin zone, while the direct bandgap lies in point-K. The indirect and direct bandgap transition observed in MoS_2 when shifted from bulk to monolayer is due to quantum confinement effects [4].

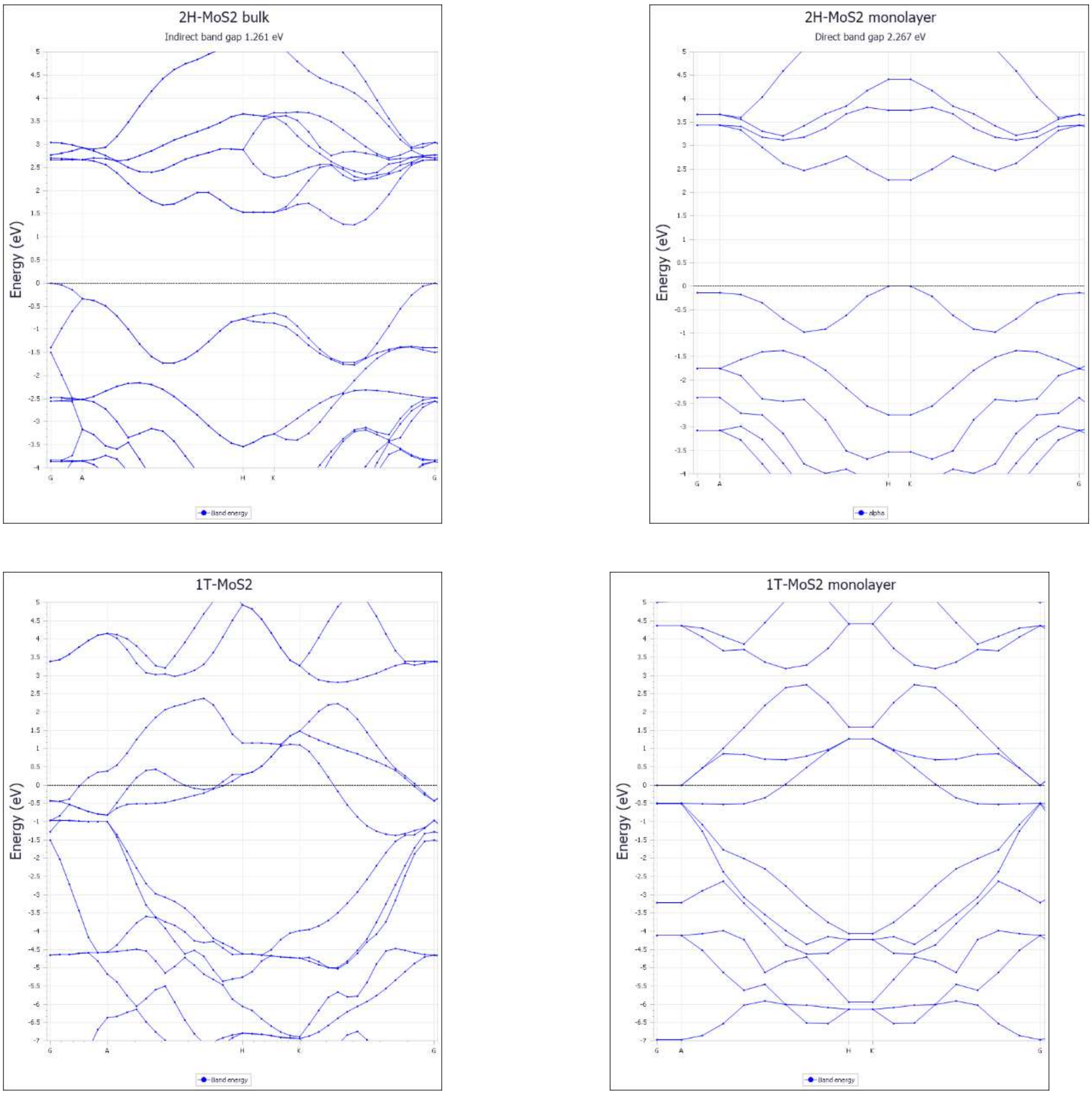

(a) (b)

Figure S3: DFT band structure calculations using hybrid functional code, (a) and (b) electronic band structure diagram of bulk and monolayer MoS_2.

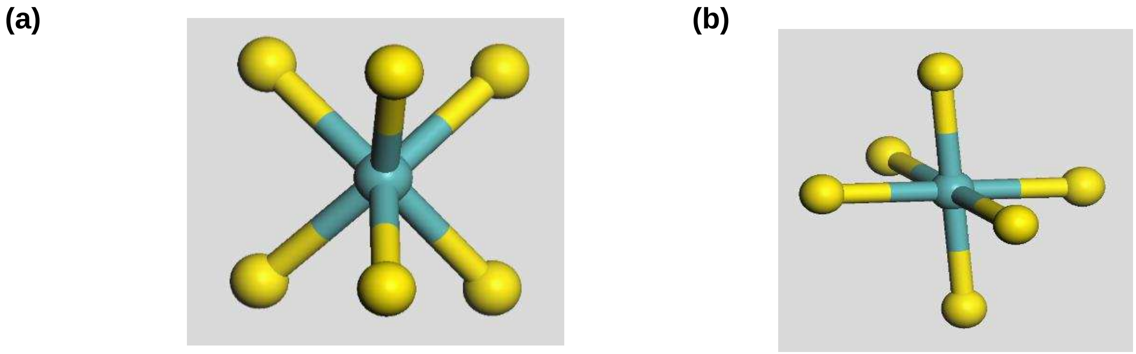

Figure S4: The DFT modelled 2H MoS$_2$ structure, showing (a) trigonal prism, and b) metastable octahedral 1T co-ordination.

Nonlinear Z-scan:

To measure the nonlinear optical response of the thin films, we have employed a conventional open-aperture Z-scan setup which measures the total transmittance as a function of incident laser intensity. In our Z-scan experiment, 120 fs pulses from a Ti-Saphire amplifier was used to excite the sample. The low repetition rate was kept at 1 KHz. The beam was focused by a 20 cm focal length lens, and the sample was moved along the z axis of the beam by using a computer controlled translation stage. The Rayleigh length (Z$_0$) and the beam waist in our experiment were 1.7 mm and~19 μm, respectively.

References:

1. G. Eda, H. Yamaguchi, D. Voiry, T. Fujita, M. Chen, M. Chhowalla. Nano Lett. 11, 5111, 2011.
2. G. Ban, S. Yuan, Y. Zhao, Z. Yang, S. Y. Choi, Y. Chai, S. F. Yu, S. P. Lau, J. Hao. Adv. Mat. 28, 7472, 2016.
3. M. I. Serna, S. H. Yoo, S. Moreno, Y. Xi, J. P. Oviedo, H. Choi, H. N. Alshareef, M. J. Kim, M. M. Jolandan, M. A. Quevedo. ACS Nano. 10, 6054, 2016.
4. M. Chhowalla, H. S. Shun, G. Eda, L. J. Li, K. P. Loh, H. Zhang. Nat. Chem. 5. 263. 2013.